Bolt Beranek and Newman Inc.

** שׁשּׁ**

NASA Contractor Report 165938

REPORT NO. 4764

ON THE DESIGN AND TEST OF A LOW NOISE PROPELLER

GEORGE P. SUCCI

NOVEMBER 1981

Contract NAS1-16521

PREPARED FOR:

NATIONAL AERONAUTICS AND SPACE ADMINISTRATION
LANGLEY RESEARCH CENTER
HAMPTON, VA 23665

JUN 1982
RECEIVED
NASA STI FACILITY
ACCESS DEPT.

REPORT NO. 4764

ON THE DESIGN AND TEST OF A LOW NOISE PROPELLER

George P. Succi

November 1981

Prepared for:

National Aeronautics and Space Administration
Langley Research Center
Hampton, Virginia 23665

TABLE OF CONTENTS

ON THE DESIGN AND TEST OF A LOW NOISE PROPELLER

Introduction

An extensive review of noise and performance of general
aviation propellers was performed at MIT[1]. Research was done in
three areas: A review of the acoustic and aerodynamic theory of
general aviation propellers, wind tunnel tests of three one-
quarter scale models of general aviation propellers, and flight
test of two low noise propellers.

One of the two low noise propellers was designed and tested
at MIT and has already been described[2]. The second propeller was
designed at MIT and flight tested at OSU. The design and testing
of the second propeller is reviewed herein.

This report describes the general aerodynamic considerations
needed to design a new propeller, reviews the design point
analysis of low noise propellers, and finally, compares the
predicted and measured noise levels.

Aerodynamic Considerations

To design a fixed pitch propeller for an existing aircraft
there are two points to consider. First, the propeller must be
matched to the engine. Second, the power resulting from the
engine propeller combination must be matched to the needs of the
aircraft. Fig. 1 illustrates this problem.

In Fig. 1, the vertical axis is power and the horizontal
axis is aircraft speed. The solid black line represents the
power needed to overcome aircraft drag at any particular
velocity. This power is given by the expression:

$$P = V D$$
$$D = \frac{1}{2} \rho V^2 S C_L$$
$$C_D = C_L^2/\pi Re + C_{Do}$$
$$C_L = mg/\frac{1}{2} \rho V^2 S$$

Here

P = Power

V = Aircraft Velocity

C_D = Drag Coefficient

C_{Do} = Drag due to skin friction

C_L = Aircraft Lift Coefficient

R = Wing Aspect Ratio

S = Wing Area

e = Span efficiency

mg = Aircraft Weight

These coefficients represent, in a simplified manner, the performance of the aircraft. This performance is summarized in the drag coefficient C_D which, in turn, has two parts. C_{Do} represents the drag coefficient due to skin friction, $C_L^2/\pi Re$ represents the induced loss of a finite aspect ratio wing. Further description of these characteristics may be found in introductory aerodynamic texts[3]. For our purposes, it is sufficient to note that these coefficients were measured at OSU and are summarized in the following table.

Table 1
Aircraft Characteristics

Parameter	Value	Comment
S	13.44 M^2	144.6 ft^2 wing area
c_{Do}	.05	skin friction coefficient
R	7.415	aspect ratio
e	0.65	span efficiency
mg	9029.9 N	2030 lbs (utility weight)

The heavy dashed line in Fig. 1 represents the power
available from the production engine propeller combination, with
the engine operated at full throttle. This power is the product
of the propeller thrust times the aircraft velocity. The produc-
tion engine propeller power was deduced from two observations.
First, the fastest sea level velocity attained by the aircraft
was 63.2 M/S (141.4 mph). Second, the best rate of climb occurs
at 40 M/S (90 mph) and is approximately 4 M/S (800 ft/min).
Wherever the power available exceeds the power needed to overcome
aircraft drag, the aircraft can climb. The velocity at which the
two curves intersect is the peak forward velocity.

The acoustic design point is the full power flyover at 305 m
(1000 ft) altitude which is specified in FAR 36[4]. The acoustic
goal is to reduce the propeller noise, as measured by a ground
observer, with no loss in aerodynamic performance. Hence, the
design point is to match the propeller performance during a full
power level flyover. The procedure is to design a propeller

3

which minimizes the induced losses at the design condition.
There are six parameters needed to specify the design of a
minimum induced loss propeller. These are given in Table 2,
along with the associated values for the existing propeller.

Table 2

Propeller Design Specifications

Parameter	Existing Propeller	New Propeller	Comment
Air Density	1.225 KG/M^3	1.225 KG/M^3	Sea Level
Velocity	63.2 M/S	63.2 M/S	Max. Velocity
Rotation Rate	2700 RPM	2700 RPm	Max.Rotation Speed
Power	122 kw (164 hp)	122 kw (164 hp)	Max Eng. Pwr.
Blades	2	3	
Radius	.97 M (38")	.87 (34")	

The implied constraint is that the efficiency (85%) be
approximately the same for both. This is discussed in greater
detail in the next section.The measured properties of the new and
existing propellers demonstrated that they were identical during
a full power flyover.

However, as evident in Fig. 1, it is important to maintain
aerodynamic performance of over a range of airspeed. The
procedure used to analyze this performance is indicated in Figs.
2a, 2b, 2c. Fig. 2a represents the measured engine power versus
rotation speed on the OSU aircraft. This was given by the appro-
ximate equation

$$P = 122.3 + .0447 (X-2700)$$

4

where P is the engine power in kilowatts, and X is the engine
RPM. One point to note is that the measured peak engine power
122 kw (164 hp) is less than the rated power 134 kw (180 hp).
Fig. 2b and 2 c represent the calculated propeller
characteristics. These are given in non-dimensional form as
power coefficient ($C_p = P / \frac{1}{2}\rho n^3 R^5$) and thrust coefficient ($C_T = T / \frac{1}{2}\rho n^2 R^4$) versus advance ratio (V/ΩR). Here $\Omega = 2\pi n$, n is the
rotation rate and R the propeller radius.

The procedure for constructing these curves is given in
Reference 5. Several general points should be made. First, the
propeller is designed to support a load distribution which
minimizes the induced loss for the conditions listed in Table
2. This procedure gives load distribution which, in turn,
specifies the product of the chord times the section lift. Air-
foil sections are chosen to operate at the maximum lift to drag
ratio for the condition. In this instance the sections are NACA
64 series airfoils. Given the section lift, the chord and angle
distribution versus radius is determined. The influence of the
aircraft nacelle is accounted for approximately by assuming lower
inflow velocities near the hub.

Once the geometry of the propeller is specified, and the
airfoil section properties tabulated, it is then possible to
construct the curves given in Fig. 2b and 2c. One parameter is
absent from Fig. 2b and 2c: the propeller Mach number. The Mach
number is important because the airfoil section properties depend
on Mach number. To accomodate the effect in an approximate way,
Figs. 2b and 2c are constructed for a propeller rotating at 2700
RPM. A more accurate analysis would require a series of curves
to be constructed for each Mach number. This is more detail than
needed for a preliminary analysis.

To synthesize the engine-propeller curve of Fig. 1, follow
the steps listed in Fig. 2. First, select rotation rate from the
engine curve; this gives an engine power (Fig. 2a). Given the
power and rotation rate, find the advanced ratio at which the
propeller power absorption matches the engine power (Fig. 2b);
this gives the aircraft velocity. Now, from the advance ratio,
find the thrust produced by the propeller (Fig. 2c). The product
of this thrust times the velocity, plotted against velocity,
yields a power curve similar to that plotted in Fig. 1.

Design Point Analysis

Table 2 shows that the new propeller differs from the old
propeller in that it has three blades and a reduced diameter.
The strategy is to combine two noise reduction methods in such a
way that the efficiency is maintained. This strategy is based on
methods developed for reducing noise on the MIT aircraft[6]. This
aircraft is similar to the OSU aircraft in that the propeller
diameter and rotation speed are identical. The largest
difference is that the MIT aircraft has a 150 hp engine, whereas
the OSU aircraft has a 180 hp engine. However, the similarities
outweigh the differences and the same design charts used for the
MIT aircraft were used for the OSU aircraft.

The goal is to minimize the peak dBA levels recorded by a
ground observer as the aircraft flies a level path at an altitude
of 304.8 meters. The test condition must be in accord with those
specified in FAA Advisory circular 36-1A(a). Appendix F, Section
36.111, paragraph 6 states "Over flight must be performed at
rated maximum continuous power." In accordance with this regula-
tion, the design point is top speed at full power at the red line
RPM. The maximum sound level on the ground occurs when the

aircraft is 5° past the zenith. This is the point at which the sound is computed in the design charts.

In Fig. 3a and 3b the effect of changing the number of blades is examined. Fig. 3a illustrates the effect on propeller efficiency. The figures were constructed by designing a series of minimum indiced loss propellers. As the number of blades increases, the efficiency increases and both the sound level decreases at a slower rate than the unweighted sound level because the blade passing frequency increases with the number of blades.

The noise is changed by altering the source strength. Compare a two and three blade propeller, each of which absorbs the same power. A blade of the two blade propeller must provide 1 ½ times more force than a blade of a three blade propeller and must have, approximately, a chord 1 ½ times as large. Because the peak sound level is dominated by conditions on a single blade, this fact means that the source strength for both the thickness and loading terms must be larger on the propeller with fewer blades.

In Fig. 4a and 4b the effect of altering the radius is examined. Fig. 4a illustrates the effects on sound level, Fig. 4b illustrates the effects on propeller efficiency. (Once again, the figures are constructed by designing a series of minimum induced loss propellers.)

The horizontal axis is the propeller radius as a percentage of the production propeller radius. As the radius increases the efficiency increases and both the sound level and A-weighted level increase. The noise is changed by altering the tip

7

speed. Because the rotation is fixed at 2700 RPM, the tip speed
is directly proportional to the propeller radius.

The two noise reduction strategies were combined as
follows: A minimum induced loss propeller was designed with the
characteristics of the production propeller listed in Table
2.Next, a second propeller was designed with three blades. This
change reduced the sound level and increased the efficiency.
Finally, the radius of the three blade propeller was reduced to
90% of the original value. This further reduced the noise and
reduced the efficiency down to its original value. An off-design
analysis showed that this propeller would operate approximately
the same as the original. This meant that it would be quieter
than the original propeller for all flight velocities. Its tip
speed would always be lower, because of the smaller radius, and
the source strength would always be 2/3 of that of a comparable
two blade propeller.

Data Review

OSU has flight tested the low noise propeller. Aerodynamic
observations indicate no degradation in performance at the design
point. That is, at full throttle during level flight, the engine
rotated at 2700 RPM and the aircraft flew at the same airspeed.

Acoustic comparison of the new and old propellers is given
in Fig. 5. The horizontal axis in flight speed and the vertical
axis is the sound level measured with a wing-mounted
microphone. This microphone was mounted in the disk plane at
1.90 (6.22 ft) from the propeller axis. The measurements were
taken at several airspeeds during level flight at 1524M (5000 ft)
altitude. At all flight speeds the new propeller is four to six

8

dB quieter than the old. Also listed on the figure is the
difference in noise level of the old propeller with and without a
muffler attached to the engine. That the noise level was reduced
after attaching the muffler indicates the engine is also an
important noise source for this aircraft.Nontheless, the engine
noise problem was easily suppressed, and propeller alterations
yielded still further noise reductions.

Figure 6 compares the predicted and measured sound levels
for the new propeller. The sound level measured with the wing
mounted microphone is compared to predictions for a range of
flight speeds. The predictions were made given only the shape and
motion of the propeller, no empirical adjustments were made. The
first step is to calculate the propeller loads using the lifting
line theory described in Reference 5. Next, the sound field is
calculated using the known propeller shape, motion and load
distribution. In Figure 6, the measurements include all noise
sources. Better agreement is obtained if the measurements are
processed to extract the propeller noise. This procedure, w¹
is developed in Appendix A, is to compute the measured value
from the Fourier spectra. The amplitude at each propeller
harmonic is measured with a caliper. These harmonic amplitudes
are then added logarithmically to give the measured SPL.
Agreement to 1dB is possible at all flight speeds.

Figure 7 compares the measured at predicted Fourier spectra
for the high speed flight. Only the blade passing harmonics are
shown. The figure indicates that the spectra is predicted
accurately. Other comparison and a discussion of the background
noise are found in Appendix A.

Figure 8 compares the measured and predicted pressure time

signatures for th high speed flight. Again measurement and
predictions agree. However, some systematic differences are
apparent. The predicted negative amplitude exceeds the measured
amplitude for the first and fourth pulse in Fig. 8. This
indicates that one blade emits slightly less noise than the
others. Errors in the blade angle setting were recorded by OSU.
Hence, the small negative sourd pulse is most likely due to a
smaller blade load.

Conclusions

Flight tests on a new low noise propeller have demonstrated
that this propeller is 4 to 6 dB quieter than the production
propeller with no measureable reduction in aerodynamic
performance. This propeller was designed using procedures
developed at MIT during a study of the noise and performance of
propellers for light aircraft.

A comparison of the calculated acoustic signature to the
measured signature shows that the theory accurately describes the
noise from the new propeller. This study demonstrates that the
technology is now available for the control of noise in general
aviation propellers.

AERODYNAMIC DESIGN CONSIDERATIONS

FIGURE 1.

SYNTHESIS OF ENGINE
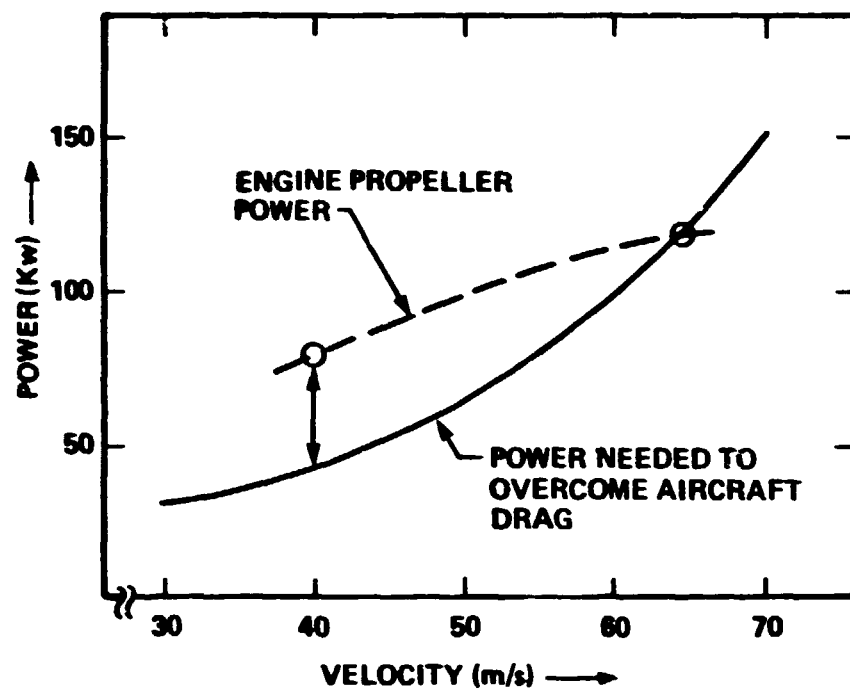## PROPELLER CHARACTERISTICS
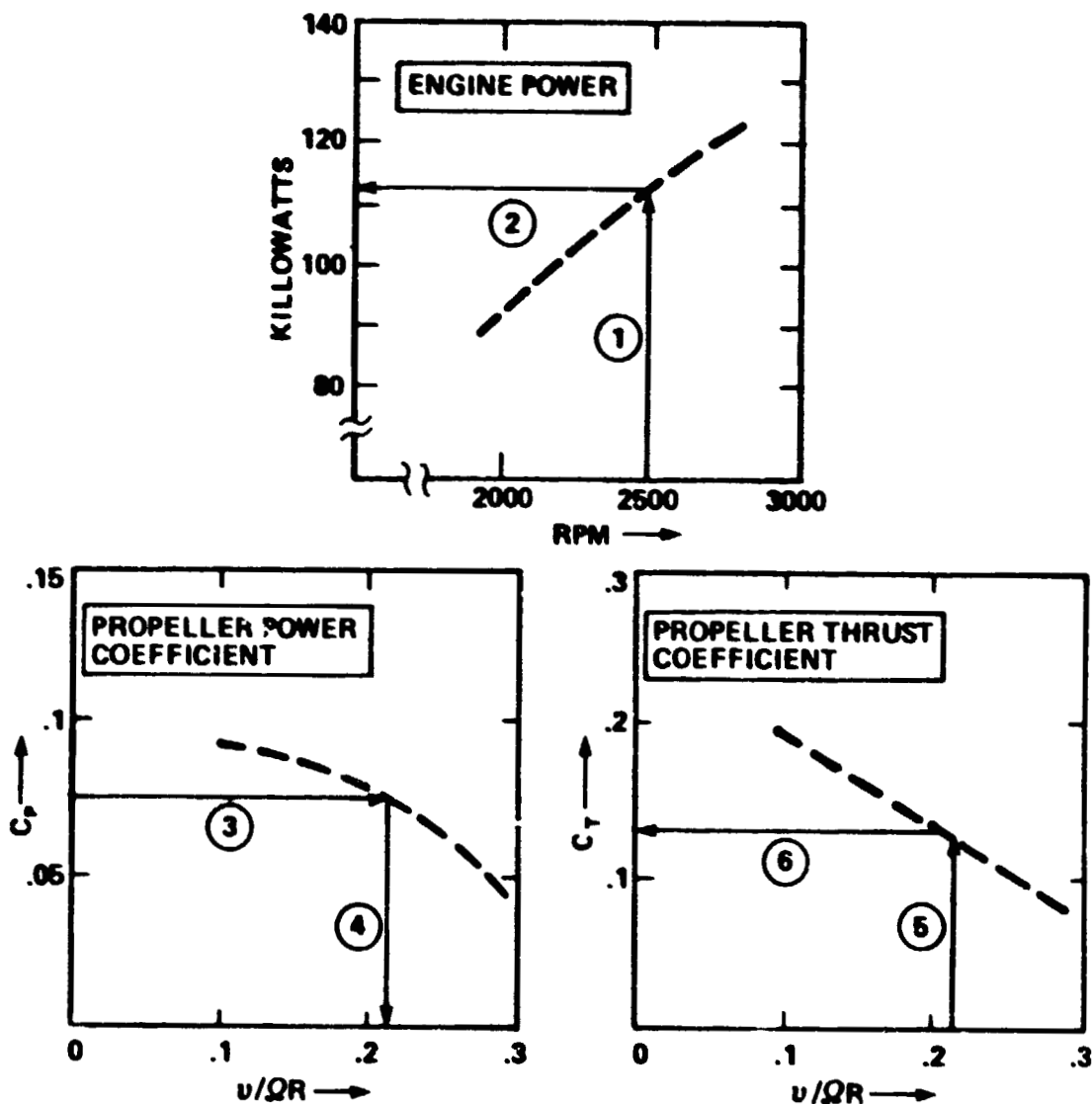
FIGURE 2.

PROPELLER DIAMETER EFFECTS
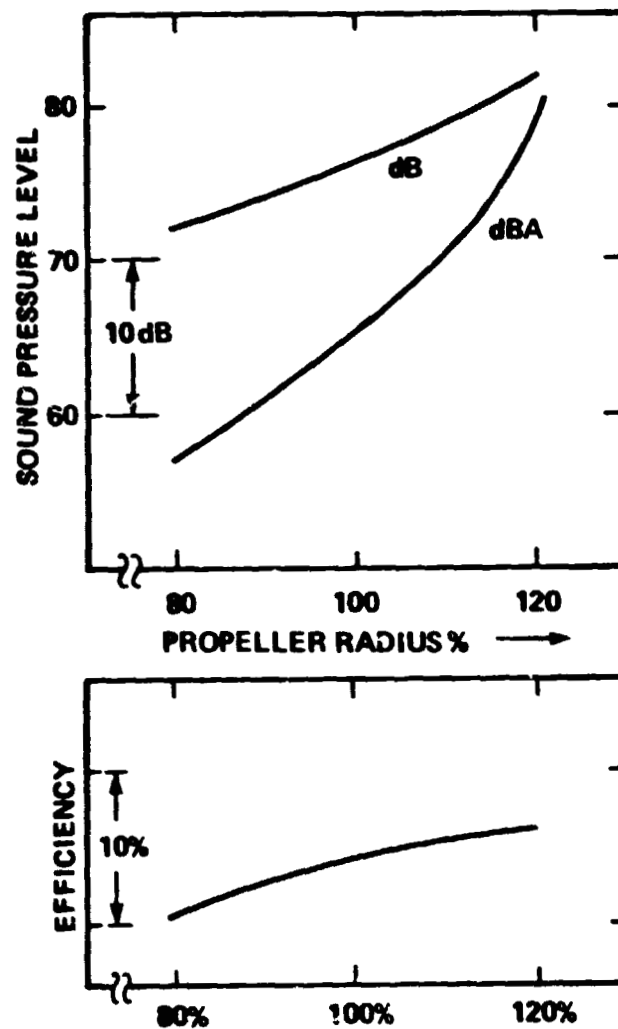
FIGURE 3.

BLADE NUMBER EFFECTS

FIGURE 4

14

FIGURE 5.

The figure is a graph titled with axes:
- Horizontal axis: Velocity (ft./sec.), ranging from 105 to 185
- Vertical axis: Sound Pressure Level (dB - Re 2x10⁻⁵ N/m.²), ranging from 111 to 123

Legend:
Disc Plane - 1.9304 m.
○ Baseline
□ Baseline With Muffler-Stack
△ MIT 3Blade With Muffler-Stack
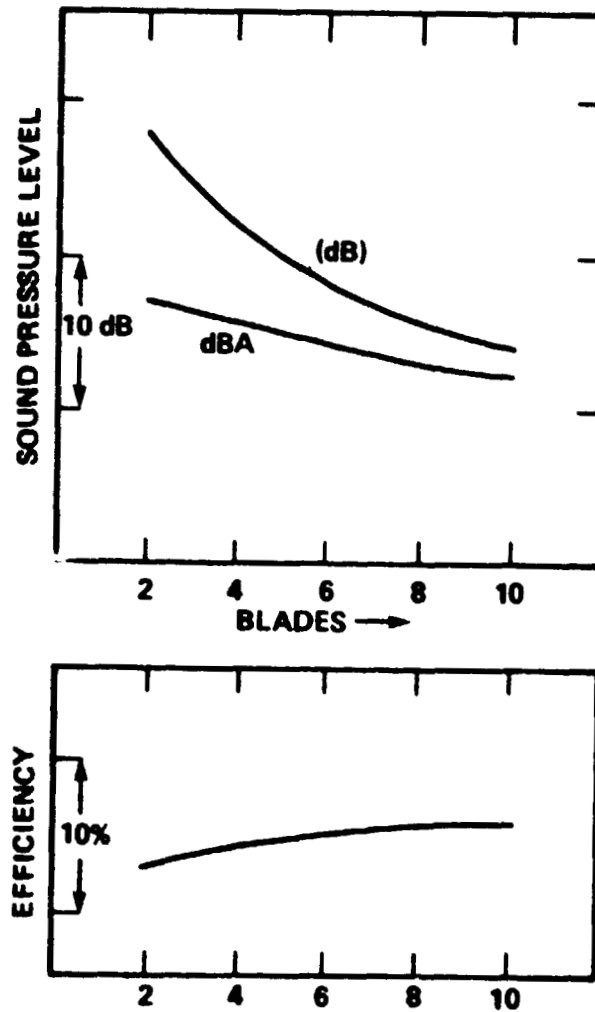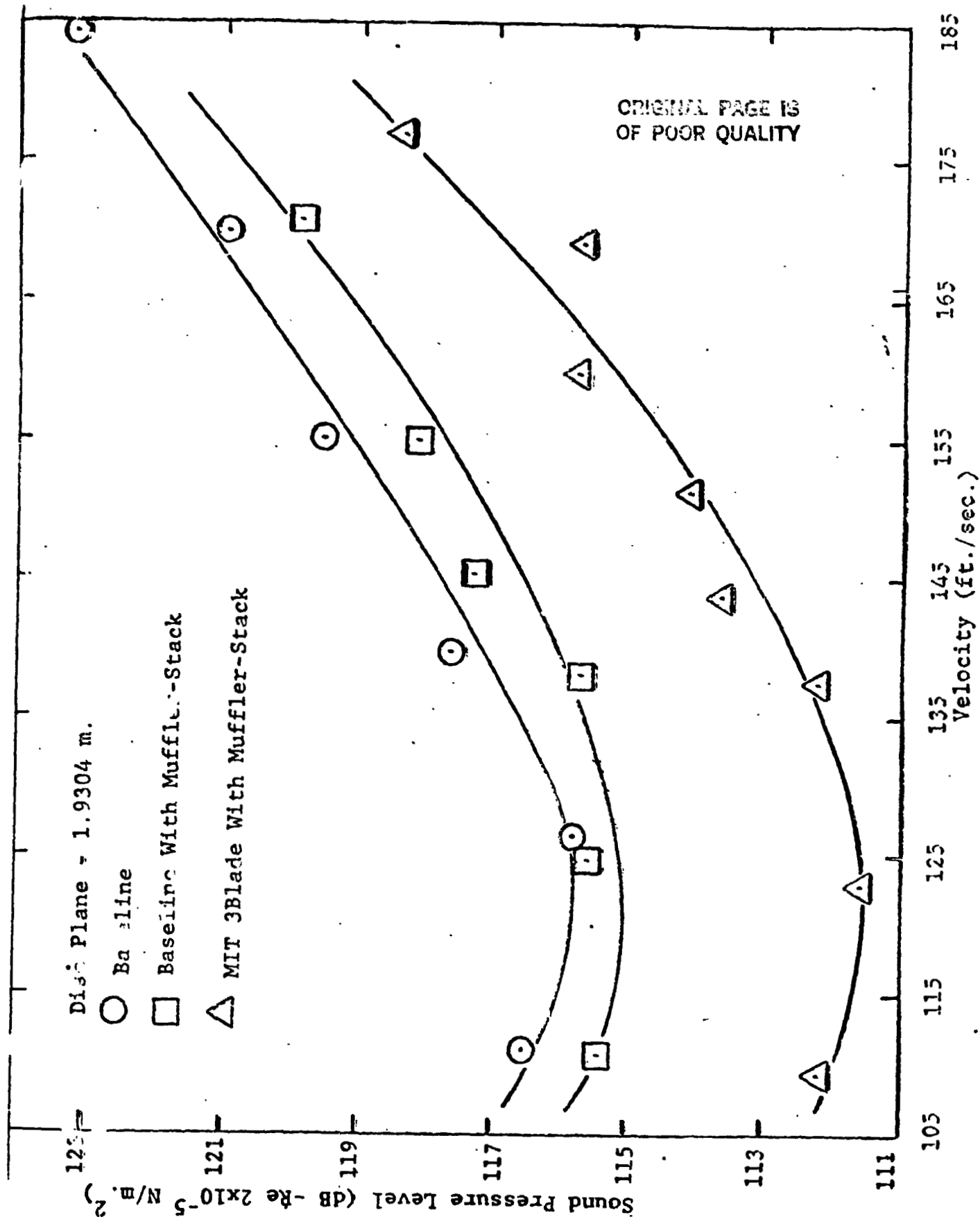
ORIGINAL PAGE IS
OF POOR QUALITY

MEASURED AND PREDICTED SOUND PRESSURE LEVELS
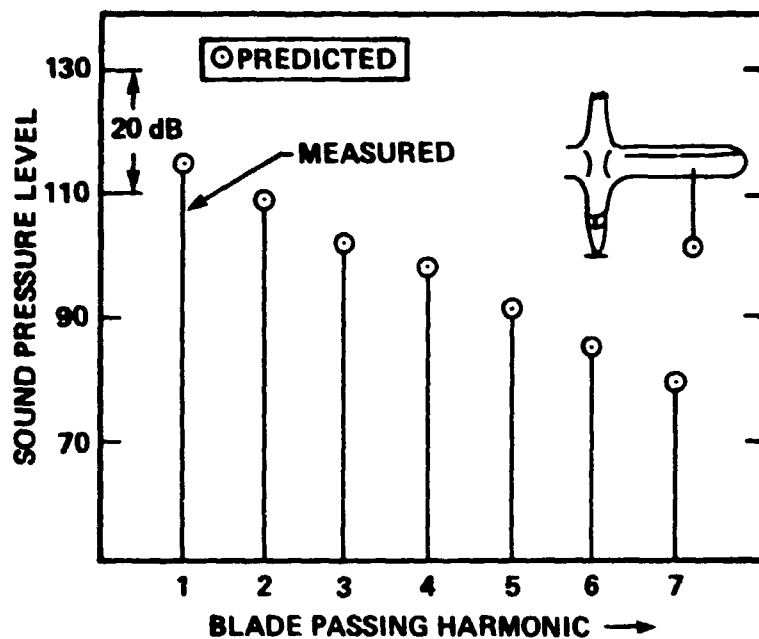

FIGURE 6

MEASURED AND PREDICTED
FOURIER SPECTRA

FIGURE 7

Boly Beranek and Newman Inc.

MEASURED AND PREDICTED
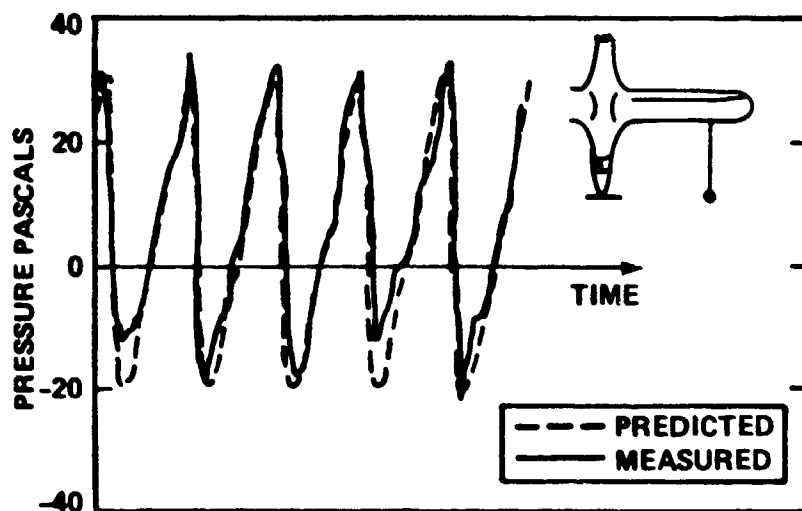## PRESSURE SIGNATURE

FIGURE 8

APPENDIX A

FURTHER COMPARISONS OF MEASUREMENT TO THEORY

Ohio State has summarized their acoustic observations for
two flights. On flight 30, the MIT propeller was set at approxi-
mately 0.2° less than its nominal pitch; on flight 34, the MIT
propeller was set at approximately 2.0° less than its nominal
pitch. During each flight a number of runs were made. Each run
corresponds to a particular aircraft velocity. A summary of
flight conditions is given in Tables A1 and A2.

Information on the sound level is also given in these
tables. The column labeled "Overall SPL" contains the
information supplied by OSU. The column : .beled "Measured
Propeller SPL" is computed at BBN. The height of each propeller
harmonic amplitude given in the Fourier spectra is measured with
a caliper. The harmonic amplitudes are then added
logarithmically to give the measured SPL. The column labeled
"Calculated Propeller SPL" contains the predicted sound levels
computed at BBN.

The overall SPL exceeds the measured propeller SPL in Table
A1 and A2 because of the influence of background noise. There is
one significant exception to this rule. These are for flight 34,
run 134 rule. In this instance the measured propeller SPL
exceeds the overall SPL. This is probably due to plotter
error. This is also the only run in which the measured spectra
exceeds the calculated spectra by a significant amount.

Figure A1 is an example of the measured Fourier spectra.
Superimposed on this figure is a line indicating the engine

A-1

harmonics. The propeller harmonics are labeled P_1. The MIT
propeller has three blades, hence the fundamental blade passing
frequency is three times the shaft frequency. The engine has
four cylinders, each cylinder fires at one half the shaft
frequency, hence the fundamental engine frequency is twice the
shaft frequency. The engine and propeller harmonics are
identical at every other propeller harmonic starting with P_2. Of
particular interest is a second set of harmonics labeled I_1.
Each of these is at the propeller frequency minus the shaft
frequency. Not all of these harmonics correspond to engine
harmonics. In particular I_2 and I_4 are neither propeller nor
engine harmonics. That the second, fifth and ninth engine
harmonics are buried in the noise indicates that the sequence of
peaks labeled I_1 (for interaction harmonic) constitute a separate
phenomena. One possible cause of these interaction harmonics is
a non linear interaction between the sound from the engine and
the sound from the propeller. This interaction can yield
additional tones at sums and differences of the engine and
propeller frequencies.

Figures A2 to A17 compare the measured and predicted
acoustic spectra. Close agreement is evident in all cases except
for run 134 (Fig. A17). The predictions were made given only the
shape and motion of the propeller. First the blade loads were
calculated, then the acoustic signature was calculated. No
empirical adjustments are needed.

Report No. 4764

Bolt Beranek and Newman Inc.

FLIGHT 30
AIR DENSITY 1.065 kg/M^3
SOUND SPEED 333 m/s
ALTITUDE 1524M

Run	Velocity	Rotation Rate	Aircraft Weight	Overall SPL	Measured Propeller SPL	Calculated Propeller SPL
	m/s	RPM	Nt	dB	dB±1	dB
119	48.86	2697	10715	118.4	117.3	117.0
120	51.30	2546	10706	115.9	115.0	113.9
121	48.68	2524	10697	115.8	113.2	113.9
122	46.12	2400	10689	114.1	112.9	112.0
123	43.86	2425	10680	113.6	114.6	111.6
124	41.91	2259	10671	112.2	110.1	110.3
125	37.52	2258	10662	111.6	110.2	110.6
126	33.38	2282	10653	112.2	110.4	111.4

TABLE A1

Report No. 4764

Bolt Beranek and Newman Inc.

FLIGHT 34
AIR DENSITY 1.076 kg/M^3
SOUND SPEED 333 m/s
ALTITUDE 1524 M

Run	Velocity	Rotation Rate	Aircraft Weight	Overall SPL	Measured Propeller SPL	Calculated Propeller SPL
	m/s	RPM	Nt			
127	55.08	2779	10800	119.1	117.3	115.6
128	52.09	2669	10791	117.7	115.8	114.1
129	49.32	2548	10782	115.5	114.9	112.4
130	47.73	2532	10773	115.4	114.8	112.4
131	44.53	2449	10764	113.7	112.2	111.5
132	42.89	2352	10755	112.6	112.3	109.9
133	38.47	2316	10746	111.8	110.9	110.0
134	34.41	2265	10737	112.1	114.6	109.6

TABLE A2

FIGURE A-1

12-18-80
RUN NO. 119
FUND FREQ= 134.9HZ
SPL= 118.4 DB (MEASURED)
⊙   THEORY
.5 HERTZ BANDWIDTH

FIGURE A-2

A-6

Bolt Beranek and Newman Inc.

12-18-80
RUN NO.   120
FUND FREQ=   127.3HZ
SPL=   115.9 DB(MEASURED)
⊙ THEORY
.5 HERTZ BANDWIDTH

FIGURE A-3

Bolt Beranek and Newman Inc.

12-18-80
RUN NO. 121
FUND FREQ= 126.2HZ
SPL= 115.8 DB (MEASURED)
⊙ THEORY
.5 HERTZ BANDWIDTH

FIGURE A-4

Bolt Beranek and Newman Inc.

12-18-80
RUN NO. 122
FUND FREQ= 120.0HZ
SPL= 114.1 DB (MEASURED)
⊙ THEORY
.5 HERTZ BANDWIDTH

FIGURE A-5

11-11-80
RUN NO.   123
FUND FREQ=   117.3HZ
SPL=   113.6 DB (MEASURED)
⊙ THEORY
.5 HERTZ BANDWIDTH

FIGURE A-6

12-18-80
RUN NO.   124
FUND FREQ=   113.0HZ
SPL=   112.2 DB (MEASURED)
⊙ THEORY
.5 HERTZ BANDWIDTH

FIGURE A-7

Bolt Beranek and Newman Inc.

12-18-80
RUN NO. 125
FUND FREQ= 112.9HZ
SPL= 111.6 DB (MEASURED)
⊙ = THEORY
.5 = HERTZ BANDWIDTH

FIGURE A-8

12-18-80
RUN NO.   126
FUND FREQ=   114.1HZ
SPL=   112.2 DB(MEASURED)
⊙THEORY
.5 HERTZ BANDWIDTH

FIGURE A-9

FIGURE 10

Bolt Beranek and Newman Inc.

12-18-80
RUN NO. 128
FUND FREQ=   127.6HZ
SPL=   117.7 DB (MEASURED)

⊙ THEORY

.5 HERTZ BANDWIDTH

FIGURE A-11

Bolt Beranek and Newman Inc.

12-18-80
RUN NO. 129
FUND FREQ= 126.3HZ
SPL= 115.5 DB (MEASURED)
⊙ THEORY
.5 HERTZ BANDWIDTH

FIGURE A-12

12-18-80
RUN NO.   130
FUND FREQ=   126.5HZ
SPL=   115.4 DB (MEASURED)
⊙ THEORY
.5 HERTZ BANDWIDTH

FIGURE A-13

Bolt Beranek and Newman Inc.

ORIGINAL PAGE IS
OF POOR QUALITY

12-18-80
RUN NO.   131
FUND FREQ=   121.0HZ
SPL=   113.7 DB (MEASURED)
⊙ THEORY
.5 HERTZ BANDWIDTH

FIGURE A-14

Bolt Beranek and Newman Inc.

**ORIGINAL PAGE IS
OF POOR QUALITY**

12-18-80
RUN NO.   132
FUND FREQ=   115.8HZ
SPL=   112.6 DB (MEASURED)
⊙ THEORY
.5 HERTZ BANDWIDTH

FIGURE A-15

12-18-80
RUN NO.   133
FUND FREQ=   113.7HZ
SPL=   111.8 DB (MEASURED)
⊙ THEORY
.5 HERTZ BANDWIDTH

FIGURE A-16

Bolt Beranek and Newman Inc.

**ORIGINAL PAGE IS
OF POOR QUALITY**

12-17-80
RUN NO. 134
FUND FREQ= 113.2HZ
SPL= 112.1 DB (MEASURED)
⊙ THEORY
.5 HERTZ BANDWIDTH
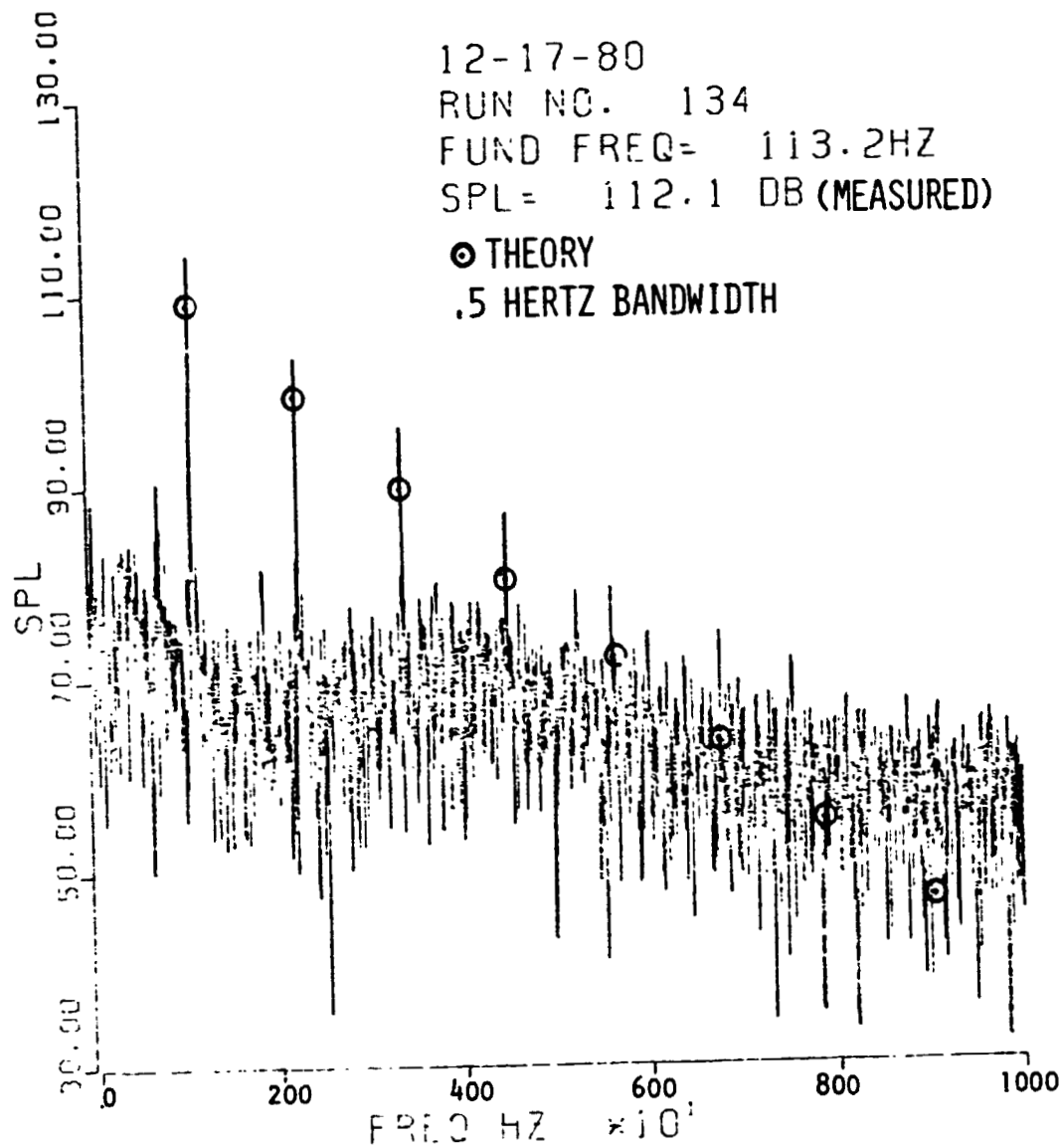
FIGURE A-17

APPENDIX B

NOTES ON THE DATA

Ohio State has spent some time developing a data package to summarize the flight test measurements. For each run a packet of information is supplied. This packet consists of two tables and three graphs. There are some small inconsistencies in this information package which are reviewed here.

Tables B1 and B2 are supplied by OSU for each run. Table B1 summarizes the engine operating conditions. Table B2 summarizes the frequency spectra. On Table B1 there are several propeller rotation rates indicated: 2700, 2541, and 2697 RPM. The first rate is the approximate reading of the flight engineer, the second rate is the tachometer reading and the last rate $_{\perp}$s that deduced from the Fourier spectra. In all the BBN calculations, only the rate deduced from the Fourier spectra is used.

Table B2 contains two sets of measurements. One set gives the computed harmonic amplitudes using an FFT routine, the second set gives the results of a real time spectrum analyzer. The results of the FFT do not agree with the spectrum analyzer. Furthermore, the tabulated data appears to be the peak amplitude at each harmonic and not the RMS amplitude.

Let A be the amplitude of the ith harmonic given in Table B2. If the sound level is $20 \log (A_i/2 \times 10^{-5})$, then this sound level exceeds that given in the plotted spectra by approximately 3 dB. Because 3 dB is approximately $20 \log 2$, the amplitudes listed in Table B2 are most probably the peak amplitudes at each harmonic.

Three figures are also supplied with each run. Fig. Bl is a
plot of the peak sound level at each harmonic. This is a plot of
the column labeled FASTFT in Table B2. Fig. B2 is a plot of the
sound level versus frequency. Each of the peaks in Fig. B2
labeled P_1 is a propeller harmonic. These peaks are 20 log
$(A_1/ 2 \times 10^{-5})$ where A_1 is the amplitude listed in Table B2.
Fig. B3 presents the pressure time signature.

There appears to be two errors in the time signature.
First, if the period is measured with calipers then the measured
period is .0235±.002 sec, which corresponds to a rotation rate of
approximately 2541 RPM. However, the measured blade passing
frequency in Fig. B3 is 136±4 Hz which corresponds to a rotation
rate of approximately 2697 RPM. This is a 6% error. Apparently
the pressure time signatures are based on the tachometer RPM.
Because the tachometer reading is suspected to be in error, the
period should be corrected as is done in Fig. 8 of this test.

The second error in the measured pressure time signature is
the sign of the amplitude. The pressure signature in Fig. B3
shows a slow drop in pressure followed by a steep rise. Also,
the peak negative amplitude is larger than the peak positive
amplitude. The calculated pressure signature shows precisely the
opposite effect. In the calculation a slow rise in pressure is
followed by a steep drop. Also the peak positive amplitude is
larger than the peak negative amplitude. The error is one of
sign, and the data can be corrected by multiplying all measure-
ments by -1. The probably source of error is the interpretation
of the voltage reading from the microphone. For condensor micro-
phones a negative voltage corresponds to a positive pressure.
This correction is also made on Fig. 8 in this test.

NASA LANGLEY ACOUSTIC MEASUREMENTS

RUN NUMBER 11 DATA REDUCED ON 12-18-80   AT 16.13

RUN NOTE: WIT PROP IN DISC PLANE FULL THROTTLE (IAS=117 MPH)

PROPELLER FLOWN HAD 3 BLADES

     CALIBRATION DATA USED:

                        SLOPE (UNITS/VOLT)   ZERO (VOLTS)   REF VALUE

MANIFOLD PRESSURE   -0.141730E+02   0.002   0.293E+02
DYNAMIC PRESSURE   -0.405700E+00   -0.032   0.000E+01
ANGLE OF ATTACK   -0.480000E+02   0.443   0.000E+01
FORWARD ACCEL   0.135000E+01   0.039   0.000E+01
RPM   0.339000E+04   -0.004   0.000E+01

MICROPHONE   0.117000E-01   0.000

PLOT SELECTIONS WERE AS FOLLOWS:

     RAW DATA PLOT F
     LIN-LIN PLOT   F
     LIN-LOG PLOT   T

TEST CONDITIONS AS KNEEPADDED:

 PRESSURE ALTITUDE 5000. FT   WITH OAT OF 497.0 DEGREES R
 AIRCRAFT WEIGHT 2409. LBS (APPROX.)
 MANIFOLD PRESSURE 24.5 IN HG   RPM 2100.

 SENSED PARAMETERS:

 MANIFOLD PRESSURE 24.0 IN HG   RPM 2541.
 DYNAMIC PRESSURE 0.184 PSI ∠TAS= 160.3 FT/SEC   DENSITY= .002066 SL/FT**3
 RAW ANGLE OF ATTACK 69.3 DEGREES
 FORWARD ACCEL 0.03 G SPEED OF SOUND= 1092.7 FT/SEC

 MICROPHONE DATA SAMPLE RATE WAS 2000.0 SPS

 CALCULATED FUNDAMENTAL FREQUENCY IS 134.9 HZ CALC RPM= 2697.
      WITH AN RMS OF THE PERIOD OF 0.251105E-03 SECONDS

 RESULTING SOUND PRESSURE LEVEL IS 118.4 DB

 VOLTAGES FROM MIC WERE AMPLIFIED BY 5.00 PRIOR TO DIGITIZING

                            TABLE B-1

Bolt Beranek and Newman Inc.

ORIGINAL PAGE IS
OF POOR QUALITY.

RESULTS OF FULL TRANSFORM AGAINST FFT FOR RUN

HARMONIC #	FREQUENCY	FASTFT	FULLFT	FREQUENCY
1	0.13477E+03	0.197E+02	0.199E+02	0.13567E+03
2	0.26953E+03	0.762E+01	0.842E+01	0.27054E+03
3	0.40430E+03	0.324E+01	0.408E+01	0.40541E+03
4	0.53906E+03	0.217E+01	0.334E+01	0.54028E+03
5	0.67432E+03	0.103E+01	0.134E+01	0.67515E+03

(PRESSURES IN N/M**2)

DB(L) = 118.35, DB(A) = 107.41, DB(B) = 115.32, DB(C) = 118.19

TABLE B-2

11-06-80
RUN NO.   119
FUND FREQ=   134.9hZ
SPL=   118.4 DB (MEASURED)

= HERTZ BANDWIDTH

FIGURE B-1

12-18-80
RUN NO.   119
FUND FREQ=   134.9HZ
SPL=   118.4 DB (MEASURED)
.5 = HERTZ BANDWIDTH
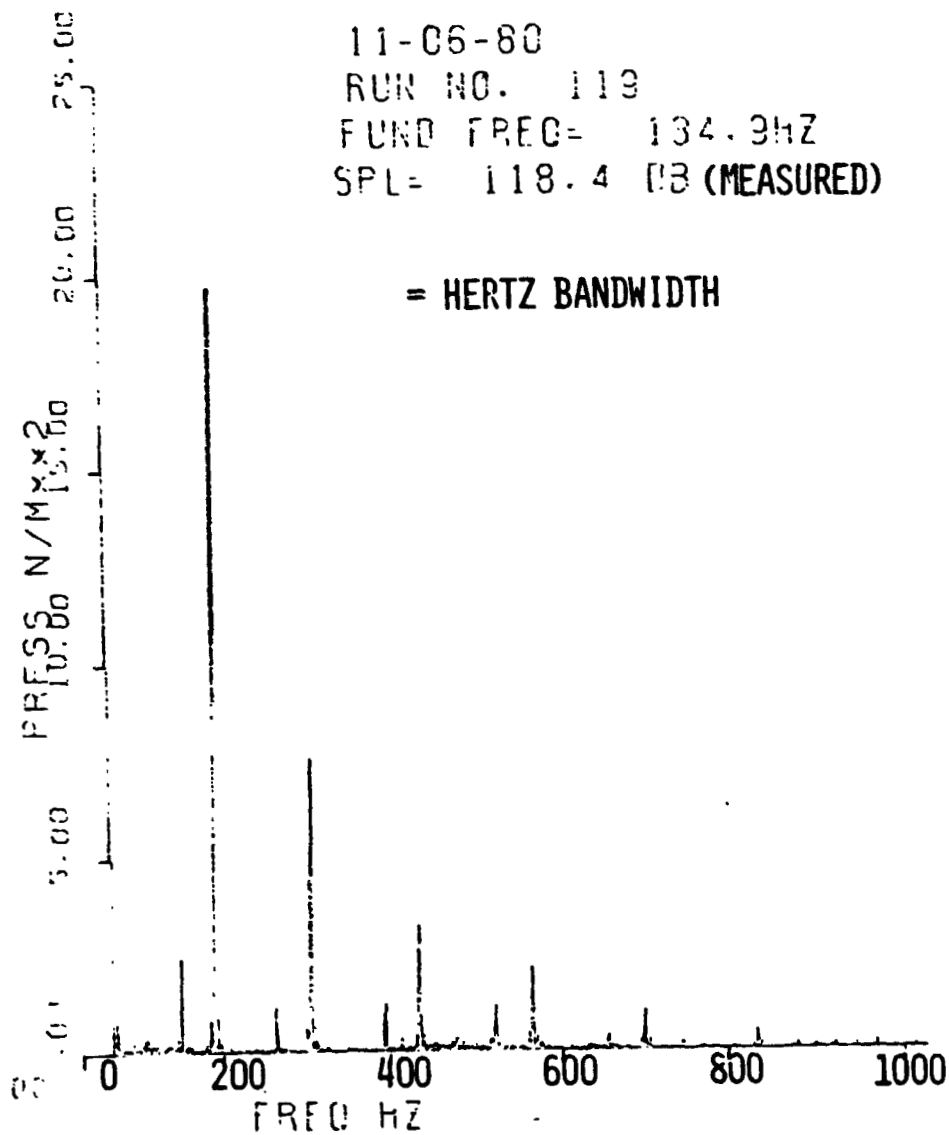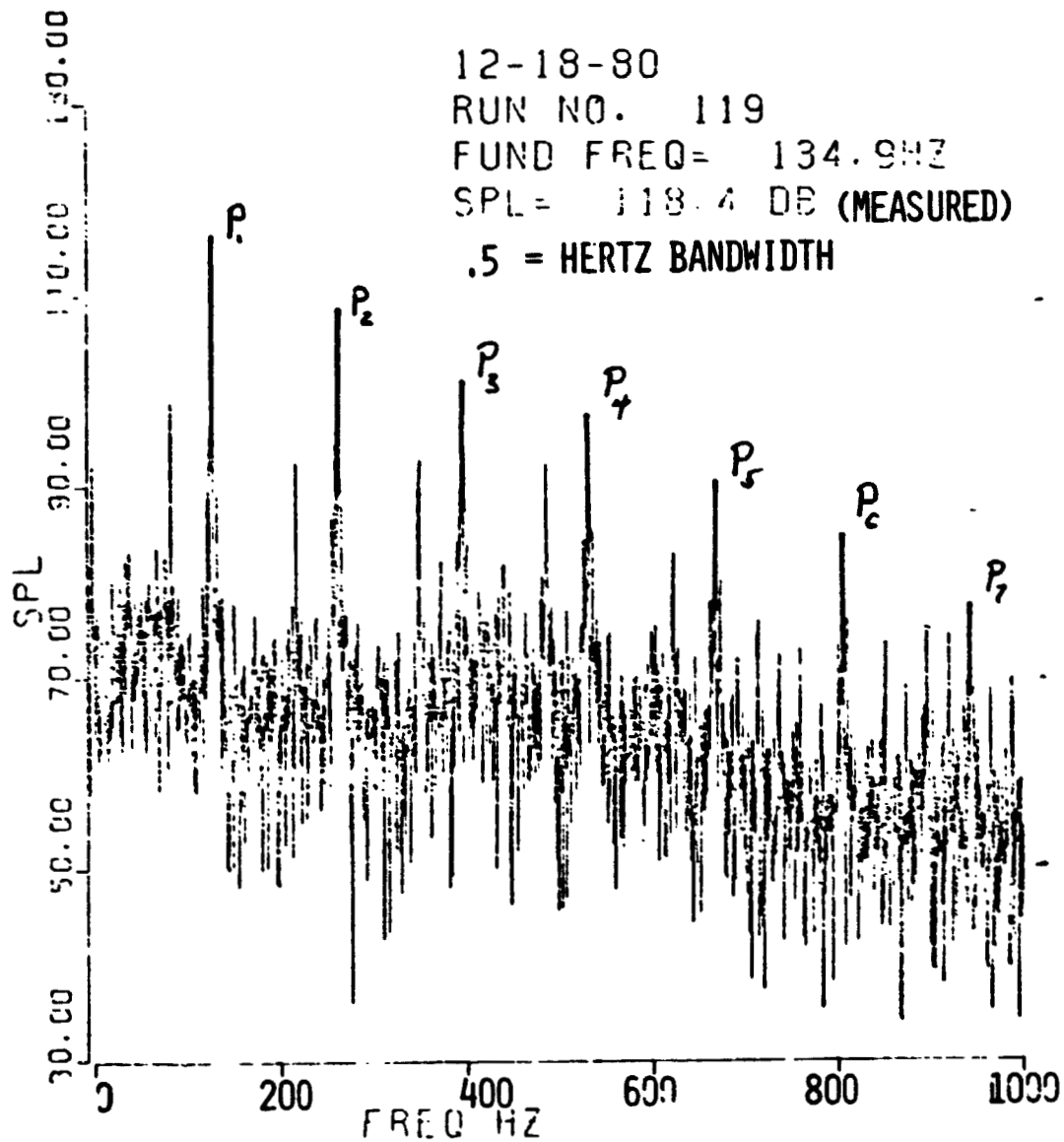
FIGURE B-2

ORIGINAL PAGE IS
OF POOR QUALITY

11-05-80
RUN NO.   119
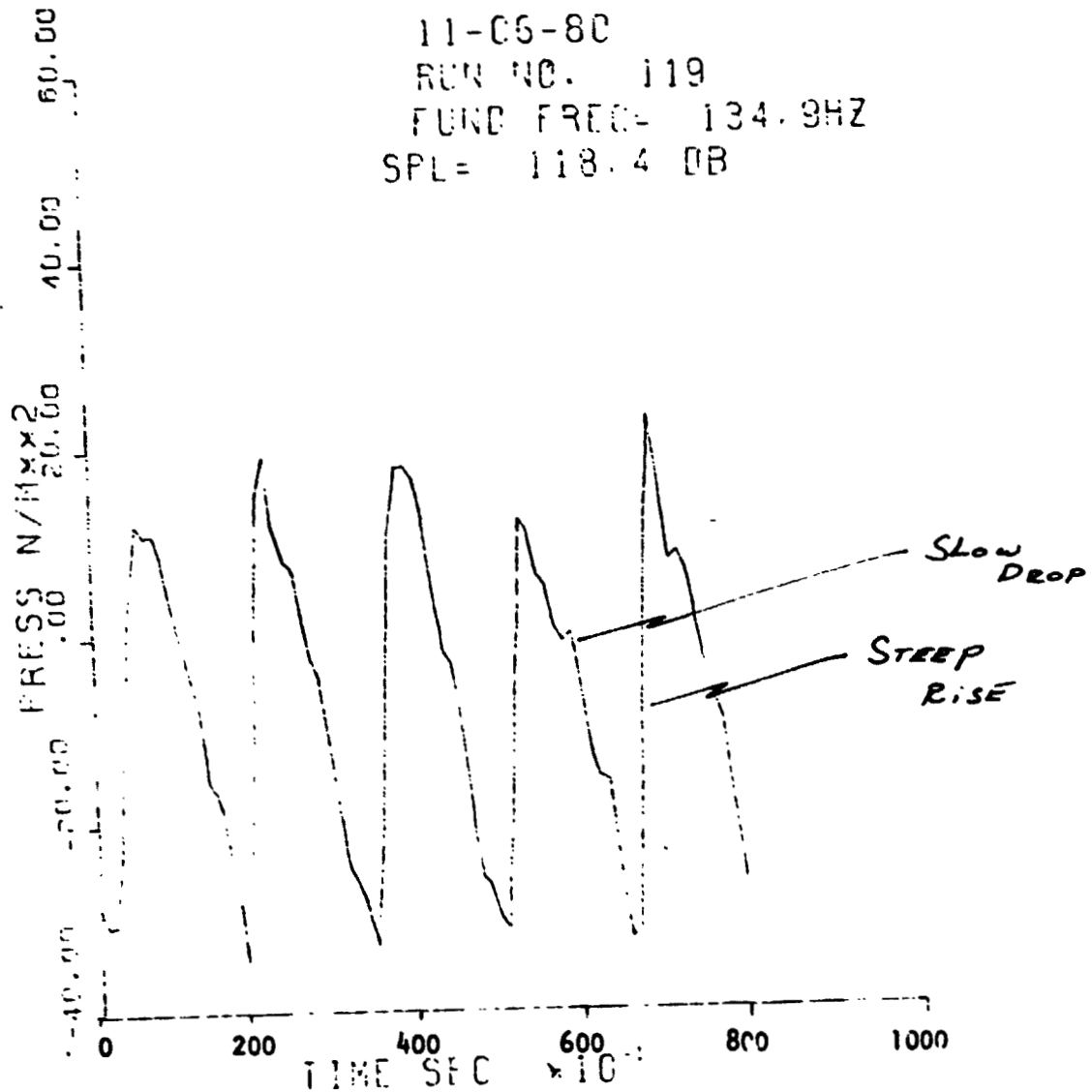FUND FREQ= 134.9HZ
SPL= 118.4 DB

FIGURE B-3

References

1. Succi, et al. "Noise Performance of Propellers for Light Aircraft" NASA CR 165732, June 1981

2. Succi, et al. "Experimental Prediction of Propeller Noise Prediction." AIAA 80-0994, June 1980

3. Houghton and Brock. "Aerodynamics for Engineering Students". Ed Arnold (Pub), London 1966

4. "Federal Aviation Noise Standards". Title 14 Code of Federal Regulations, Chapter 1, Part 36.

5. Larabee, "Practical Design of Minimum Induced Loss Propellers". SAE 790585, April 1979.

6. Succi, "Design of Quiet Efficient Propellers". SAE 790584, April 1979.